Preparation and Antibacterial Properties of Composite Films Based on PVA and Chitosan Combined with Melanin Nanoparticles

Zainal Mustakim[1,2], Agus Prasetya[1], Joko Wintoko[1], Fanny Sakinah[1], Abdul Rahman Siregar[3], Zahrul Mufrodi[4], Pandji Prawisudha[5], Kun Sri Budiasih[6], and Chandra Wahyu Purnomo[1*]

[1]*Department of Chemical Engineering, Faculty of Engineering, Universitas Gadjah Mada, Jl. Grafika No. 2, Yogyakarta 55281, Indonesia*

[2]*Department of Chemical Engineering, Faculty of Engineering, Universitas Muhammadiyah Gresik, Jl. Sumatera No. 101, Gresik 61121, Indonesia*

[3]*Microbiology Laboratory, Faculty of Biology, Universitas Gadjah Mada, Jl. Teknika Selatan, Sekip Utara, Yogyakarta 55281, Indonesia*

[4]*Department of Chemical Engineering, Faculty of Industrial Technology, Universitas Ahmad Dahlan, Jl. Jend. Ahmad Yani, Banguntapan, Bantul, Yogyakarta 55191, Indonesia*

[5]*Faculty of Mechanical and Aerospace Engineering, Institut Teknologi Bandung, Jl. Ganesha No. 10, Bandung 40132, Indonesia*

[6]*Department of Chemistry Education, Faculty of Mathematics and Natural Science, Universitas Negeri Yogyakarta, Jl. Colombo No. 1, Yogyakarta 55281, Indonesia*

* ***Corresponding author:***

email: chandra.purnomo@ugm.ac.id

Received: June 9, 2025
Accepted: August 28, 2025

DOI: 10.22146/ijc.107680

Abstract: *Developing biodegradable films with antimicrobial properties is essential for advancing sustainable packaging and biomedical applications. In this study, PVA/chitosan composite films were successfully fabricated and reinforced with melanin nanoparticles (MNPs) derived from black soldier fly (BSF) pupae waste to enhance their functional performance. The films were prepared using solution casting with varying concentrations of MNPs (0.0, 0.5, 1.0, and 2.0% w/w). FTIR analysis confirmed molecular interactions between the polymer matrix and melanin, while degradation tests showed enhanced stability due to melanin's hydrophobicity and antioxidant properties. Incorporating melanin significantly improved the films' structural integrity, surface morphology, and antibacterial activity against* Escherichia coli *and* Staphylococcus aureus*. These findings highlight the potential of PVA–chitosan–melanin composite films as promising candidates for active food packaging and biomedical applications, combining biodegradability with enhanced functional performance derived from sustainable BSF-based materials.*

Keywords: *antibacterial activity; BSF; chitosan; melanin nanoparticles; polyvinyl alcohol*

■ INTRODUCTION

The widespread environmental impact of synthetic plastic waste has driven an urgent search for biodegradable and sustainable alternatives, particularly in packaging applications [1]. The rise in global awareness regarding the environmental impacts of synthetic plastics has fueled interest in biodegradable materials, especially in agricultural and food packaging applications [2]. Biopolymer-based films have garnered significant attention due to their renewability, environmental compatibility, and potential for functional enhancement with natural additives [3-4]. Among them, polyvinyl alcohol (PVA) is a synthetic polymer known for its film-forming ability, high tensile strength, and flexibility [5-6]. However, its high hydrophilicity and lack of intrinsic antimicrobial activity limit its direct application in active packaging [6]. This necessitates the incorporation of various additives and plasticizers to enhance its performance in food packaging.

PVA and chitosan are biopolymers that have gained significant attention for their excellent film-forming capability, biodegradability, and biocompatibility [7]. PVA, a water-soluble synthetic polymer, is valued for its mechanical strength, transparency, and superior gas barrier properties, making it widely applicable in food packaging and biomedical applications [8]. Chitosan, a natural polysaccharide obtained through the deacetylation of chitin, offers additional advantages, including inherent antimicrobial activity and the ability to form stable films under acidic conditions [9]. However, chitosan films are often brittle and exhibit low mechanical strength, which can be improved by blending with PVA [7,10-11]. For instance, increasing the PVA/chitosan mass ratio from 10/90 to 50/50 raised tensile strength from 2.78 to 5.55 MPa [12]. Neat PVA films typically have tensile strengths of about 25 ± 4 MPa, which can increase to 29–35 MPa with the addition of 2–2.5 wt.% chitosan. In terms of barrier performance, water vapor permeability for neat PVA is around 10.1 g cm^{-1} s^{-1} Pa^{-1} and rises modestly to 12–15 g cm^{-1} s^{-1} Pa^{-1} when chitosan is incorporated [13].

The combination of PVA and chitosan has been widely explored to develop biodegradable films with enhanced mechanical and antimicrobial performance [7]. These hybrid films align with the growing demand for sustainable materials that can reduce reliance on conventional petroleum-based plastics [14]. Despite significant progress, the functional limitations of these biopolymer films—such as limited barrier effectiveness and lack of multifunctional properties—remain a challenge, particularly in advanced packaging and biomedical contexts where additional functionalities are desirable [11,15].

To address these limitations, recent research has investigated the incorporation of nanoparticles to enhance the properties of biopolymer matrices [16]. However, the majority of these studies rely on chemically synthesized nanoparticles, which may introduce environmental and safety concerns [17]. In this context, developing biogenic nanoparticles derived from natural or waste sources represents a more sustainable alternative [16-17].

The black soldier fly (*Hermetia illucens*, BSF), widely recognized for its role in organic waste bioconversion, offers a promising yet underutilized source of functional biopolymers [18]. The defatted biomass of BSF contains valuable compounds that can be extracted and further converted through thermochemical processes into melanin nanoparticles (MNPs) and chitosan [19]. These BSF-derived MNPs present a sustainable and value-added approach to insect waste utilization, particularly in enhancing the functional properties of biopolymer films, including antimicrobial activity [20].

Although melanin is well known for its antioxidant, UV-protective, and antimicrobial properties [21-23], the majority of research to date has focused on melanin derived from fungi and marine sources, including sepia and squid ink [19,24-26]. Melanin from sepia ink, a natural black–brown biopigment extracted from cuttlefish, has been incorporated into polymer matrices such as pectin and agar, enhancing UV shielding, hydrophobicity, mechanical strength, water vapor barrier properties, and antimicrobial efficacy—making it valuable for innovative packaging and biomedical applications [20,27]. Similarly, melanin isolated from squid ink has been incorporated into carrageenan-based nanocomposite films, improving thermal stability, UV resistance, and antimicrobial activity against foodborne pathogens [26]. Fungal melanin has also found successful applications in the cosmetics and food industries as a natural colorant and functional additive in packaging, owing to its antimicrobial properties, excellent color fastness, and non-toxicity [25].

In comparison, melanin from BSF offers distinct advantages. It is obtained from the residual biomass of large-scale insect farming and organic waste bioconversion, making it an abundant, low-cost, and sustainable feedstock [28]. Unlike fungal melanin, which requires controlled fermentation [25], or sepia ink melanin, which depends on marine harvesting [29], BSF melanin production valorizes waste streams and aligns with circular bioeconomy principles [28]. Furthermore, BSF biomass contains other high-value biopolymers such as chitosan, enabling integrated extraction processes [18]. Functionally, BSF melanin exhibits strong UV-shielding, antioxidant, and antimicrobial properties comparable to or exceeding those of fungal

and sepia ink melanin, while offering unique compatibility with nanoparticle formation [22].

Despite these advantages, the application of insect-derived melanin—particularly from BSF—in polymeric films remains largely unexplored. In this study, we report the first systematic incorporation of MNPs and chitosan extracted from BSF pupae waste into a PVA/chitosan hybrid film. This sustainable approach valorizes insect biomass and produces a biodegradable composite with improved mechanical strength, water resistance, antimicrobial activity, and biodegradability. A comprehensive evaluation of its structural, mechanical, physicochemical, antimicrobial, and degradation properties offers fresh insights into the potential of insect-based biopolymers for advancing sustainable material development.

■ EXPERIMENTAL SECTION

Materials

BSF pupae were sourced from the Agrotechnology Innovation Center, Universitas Gadjah Mada (UGM), Yogyakarta, Indonesia. *Escherichia coli* ATCC 25922 and *Staphylococcus aureus* ATCC 25923 were obtained from the Microbiology Laboratory, UGM. Analytical-grade reagents, including acetic acid, PVA, hydrochloric acid (37%), and sodium hydroxide, were procured from Sigma-Aldrich.

Instrumentation

An analytical balance and Whatman filter paper were used for weighing and filtration, while a sieve shaker and ultrasonicator supported sample preparation. Extraction utilized beakers, a heater, and a stirrer, complemented by reflux condensers, thermometers, and standard glassware such as graduated cylinders, pipettes, and Erlenmeyer flasks.

Procedure

Chitosan and melanin were extracted from BSF pupae following a conventional extraction procedure [30]. The pupae were thoroughly washed with water to eliminate surface impurities, then dried and milled into a fine powder capable of passing through a 100 μm mesh before extraction.

Extraction of chitosan and MNPs

Demineralization. Demineralization was performed for 2 h at 50 °C with continuous stirring at 200 rpm, using a raw material-to-3 M HCl ratio of 1:10 (w/v) [31]. The resulting materials were then filtered, rinsed with distilled water until reaching a neutral pH, and oven-dried at 60 °C overnight [32].

Deproteinization. Deproteinization was carried out using 2 M NaOH at a solid-to-liquid ratio of 1:10 (w/v) [33]. The suspension was stirred at 200 rpm and maintained at 80 °C for 2 h [30]. Following treatment, the mixture was filtered, thoroughly rinsed with distilled water to remove any residual NaOH and dried at 60 °C overnight [32].

Deacetylation. The deproteinized material was treated with 12 M NaOH at a solid-to-liquid ratio of 1:20 (w/v), stirred at 200 rpm, and heated to 100 °C for 2 h [30]. Upon completion, the mixture was washed with distilled water, with solids separated by filtration or centrifugation, while melanin remained in the supernatant [34]. The recovered solids were repeatedly rinsed with distilled water until a neutral pH was achieved, followed by overnight drying in an oven at 60 °C to obtain the final product with stable mass, ensuring no significant material loss during the process [32].

Purification of chitosan and MNPs

Purification of Chitosan. The deacetylated material was dispersed in 1% (v/v) acetic acid (1:100 w/v) and stirred at room temperature for 24 h [30]. The mixture was centrifuged at 6,000 rpm for 15 min, and the supernatant was collected [35]. Chitosan precipitation was induced by adjusting the pH to alkaline using 6 M NaOH, followed by overnight incubation at 4 °C [30,36]. The precipitate was recovered by centrifugation, washed with distilled water to remove residual acetate, freeze-dried, and stored at room temperature [34]. Energy-dispersive X-ray spectroscopy (EDS) analysis indicated ~93.76% purity, with carbon, nitrogen, and oxygen as the main elements.

Purification of MNPs. The melanin-containing supernatant was acidified to pH 2 with 1 M HCl to precipitate melanin [37]. The mixture was centrifuged at 6,000 rpm for 20 min [38]. The precipitate was washed

repeatedly with distilled water and centrifuged to neutral pH [39], then freeze-dried and stored at room temperature [40]. EDS analysis indicated ~62.48% purity, with carbon, nitrogen, and oxygen as the main elements. Melanin was characterized by scanning electron microscopy (SEM) and particle size analysis (PSA, Horiba SZ100 Particle Size Analyzer).

Preparation of films

Composite films were prepared via solvent casting, adapted from Roy and Rhim [27]. A 1 g of PVA was dissolved in 100 mL of 1.0% (v/v) acetic acid at 75 °C with stirring for 30 min. Melanin was then incorporated at 0.0, 0.5, 1.0, or 2.0 wt.% relative to the total PVA/chitosan weight, with concentrations selected based on literature reports and preliminary screening results. Previous studies have demonstrated that incorporating 1–5 wt.% chitosan nanoparticles into starch–PVA films significantly enhances tensile strength, water vapor barrier properties, and antimicrobial activity [41]. Similarly, PVA/starch/chitosan films reinforced with metal nanoparticles showed peak mechanical performance at around 1 wt.%, while higher loadings (2 wt.%) led to nanoparticle aggregation and reduced strength [42]. Agar-based films containing 0.25 wt.% MNPs achieved uniform dispersion without aggregation, whereas 2.0 wt.% caused particle clustering [27]. In line with these findings, our preliminary trials revealed that melanin concentrations below 0.5 wt.% had little effect on film performance. Therefore, a range of 0.5–2.0 wt.% was chosen to balance functional improvement with structural integrity.

To ensure uniform melanin dispersion, the mixture was ultrasonicated for 15 min [43]. Subsequently, 1 g of chitosan and glycerol (as a plasticizer at 30 wt.% of the combined PVA and chitosan weight) were added, and the solution was stirred at 75 °C for 1 h until fully dissolved [27]. The resulting film-forming solution was cast into silicone molds lined with Teflon sheets and dried in an oven at 60 °C for 24 h, following the method of Liang et al. [20]. The resulting PVA/chitosan/MNPs composite films were labeled as PVA/Chi, PVA/Chi/Mel$^{0.5}$, PVA/Chi/Mel$^{1.0}$, and PVA/Chi/Mel$^{2.0}$, corresponding to the respective melanin concentrations.

Characterization of PVA/Chi/MNPs composite films

Fourier transform infrared (FTIR). FTIR spectroscopy was performed on the film samples using a Shimadzu spectrophotometer equipped with an attenuated total reflectance accessory. Spectral data were acquired across the 500–4000 cm^{-1} wavenumber range, with 45 scans accumulated at a resolution of 4 cm^{-1} to ensure accurate and reproducible characterization [44].

Thickness and tensile strength of the composite films. Film thickness was measured using a micrometer with a precision of 0.01 mm [45]. Measurements were performed at five randomly selected locations on each film sample, and the average value was used for subsequent tensile strength calculations [46]. The tensile strength (TS) was evaluated using a LLOYD Instruments LR5K universal testing machine [47].

Water solubility and swelling ratio of composite films. The film samples' water solubility (WS) was assessed by calculating the percentage of dry matter dissolved after immersion in water. Three randomly selected specimens of each film type (2 cm × 2 cm) were initially dried at 100 °C for 24 h to determine their initial dry weight (W_1). The specimens were then immersed in 50 mL of distilled water for 24 h [48]. Following immersion, the films were collected and dried in an oven at 105 °C for an additional 24 h to determine the final undissolved dry weight (W_2) [47]. The WS was calculated using Eq. (1).

$$WS\% = \frac{W_1 - W_2}{W_1} \times 100\% \quad (1)$$

The films' swelling ratio (SR) was determined using a gravimetric method. Pre-weighed film specimens (2 cm × 2 cm) were immersed in distilled water for 24 h. After immersion, the films were carefully removed, and any excess surface water was gently blotted using filter paper prior to reweighing [47]. The SR percentage was calculated using Eq. (2):

$$SR\% = \frac{W_4 - W_3}{W_3} \times 100\% \quad (2)$$

where W_3 and W_4 represent the weights of the film samples before and after immersion in water, respectively.

Degradability. The degradability of the films was assessed using a soil burial test. In this method, biofilm samples were cut into 2 cm × 4 cm strips, and their initial dry weight (W_5) was recorded [49]. The samples were then buried at a depth of six inches in compost soil and incubated at room temperature for a period of 35 d, with sampling carried out at 7-d intervals. After each retrieval, the films were gently cleaned to remove any adhering soil, and the final dry weight (W_6) was measured [50]. The percentage of degradation was calculated using Eq. (3).

$$\text{Degradation}\% = \frac{W_5 - W_6}{W_5} \times 100\% \quad (3)$$

Antibacterial activity. The antibacterial activity of the composite films was assessed against foodborne pathogenic bacteria, specifically the Gram-positive *S. aureus* and the Gram-negative *E. coli* [51]. Each bacterial strain was pre-cultured under aerobic conditions in 150 mL of nutrient broth at 37 °C for 24 h. A reference for initial colony quantification of *E. coli* and *S. aureus* was 1.7×10^9 bacteria/mL and 5.1×10^8 bacteria/mL, respectively. For antimicrobial testing, 1 mL of the bacterial suspension was inoculated into 9 mL of fresh nutrient broth containing the film samples (8 × 20 mm). The mixtures were incubated under aerobic conditions at 37 °C for 24 h with moderate shaking at room temperature [52]. The antibacterial efficacy of the films was preliminarily assessed by measuring the turbidity of the culture medium, with absorbance readings taken at 600 nm using a Shimadzu spectrophotometer [53]. Antimicrobial efficiency was calculated based on turbidity data to quantitatively assess the reduction in bacterial growth as influenced by the concentration of composite films. This evaluation involved analyzing the time derivative at the maximum absorbance observed for each sample [51]. The inhibitory proportional factor (I_f) represented the ratio between the maximum bacterial growth rate in the control and the presence of composite films. Specifically, I_c and I_{cf} denote the maximum absorbance values corresponding to the control (without film) and the test medium containing composite films, respectively, measured when bacterial growth reached its peak (i.e., maximum optical density). The I_f value was calculated using Eq. (4).

$$I_f = \frac{I_c - I_{cf}}{I_c} \quad (4)$$

Statistical analysis. Each film property was measured in triplicate and presented as mean ± standard deviation (SD). Statistical analysis was performed using analysis of variance (ANOVA), with $p < 0.05$ considered the threshold for significance. Differences among mean values were further analyzed using Tukey's post hoc test in Minitab 18.

■ RESULTS AND DISCUSSION

Preparation of Films

The melanin-based composite developed in this study represents a practical and environmentally friendly material, owing to its biodegradability and the incorporation of naturally derived antioxidants sourced from waste materials. The SEM micrographs and particle distribution of melanin can be seen in Fig. 1. The melanin exhibited a relatively homogeneous and smooth surface morphology, although minor aggregations were still observable. The particle size distribution of melanin

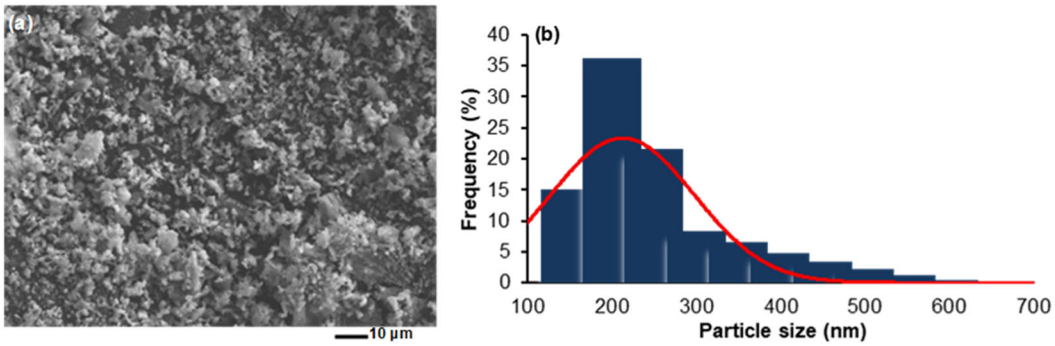

Fig 1. (a) SEM images and (b) particle size distribution histogram of the melanin

ranged from 100 to 600 nm, with an average diameter of 212.4 ± 85.5 nm. In comparison, melanin isolated from squid ink sacs and sepia ink has been reported to exhibit a spherical morphology with particle sizes typically ranging between 100 and 200 nm [27]. Nanoscale dimensions of melanin may facilitate improved interactions with bacterial membranes, thereby enhancing their antibacterial effectiveness [54].

Incorporating melanin into the PVA/chitosan matrix significantly altered the visual aspects of the composite films. As melanin content increased, the films transitioned from lighter shades to darker hues, reflecting the increase in melanin concentration, as shown in Fig. 2. Melanin's deep pigmentation imparts a distinct dark color to the films, which could have implications for applications in food packaging, where visual indicators of microbial contamination may enhance consumer safety [55]. Although transparency was not explicitly measured in this study, the observed optical changes suggest that higher melanin concentrations could lead to reduced transparency, as melanin's inherent pigmentation likely causes opacity. Future studies will directly measure the composite films' transparency values to further understand the impact of melanin content on their optical properties.

FTIR Analysis

The FTIR spectra of film samples containing PVA, chitosan, and melanin, shown in Fig. 3, reveal notable shifts in the transmittance values, which suggest specific interactions between the hydroxyl (–OH) and amine ($–NH_2$) functional groups of PVA/chitosan and the melanin structure. The increase in intensity at 3254 cm^{-1} (O–H and N–H stretching vibrations) from 68.68% in the PVA/Chi film to 77.99 and 77.69% in the PVA/Chi/$Mel^{0.5}$ and PVA/Chi/$Mel^{2.0}$ samples, respectively, indicates potential hydrogen bonding and molecular interactions [12]. These interactions may enhance the mechanical properties of the films, such as increased strength and flexibility, as hydrogen bonds are known to improve film cohesion and stability [56].

The absorption band at 2935 cm^{-1} (C–H stretching vibration of methyl groups) reflects changes in the polymer chain structure, particularly at the terminal ends of the PVA/Chi/Mel composite [57-58]. This shift may affect film flexibility and thermal stability, as modifications to the polymer chain's terminal groups influence its overall rigidity and resistance to heat [59]. Additionally, the absorption bands at 1646, 1555, and 1412 cm^{-1} correspond to the amide I, II, and III vibrations (C=O stretching, N–H bending, and C–N stretching, respectively) [30,60]. These bands, associated

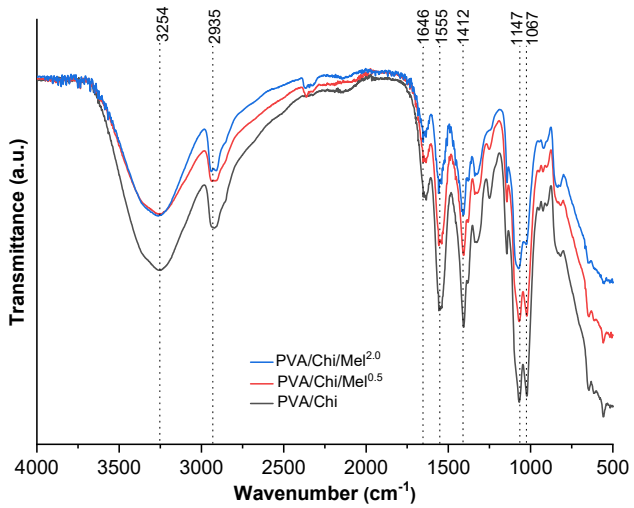

Fig 3. FTIR spectra of PVA/Chi/Mel composite films

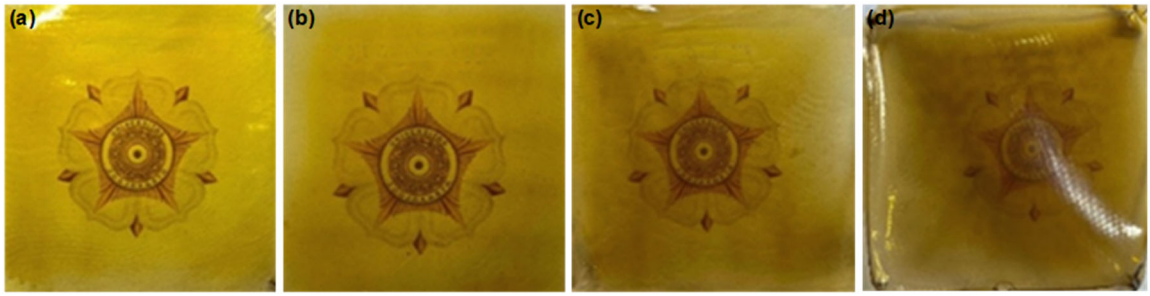

Fig 2. Visual appearance of PVA/Chi/Mel composite films: (a) PVA/Chi, (b) PVA/Chi/$Mel^{0.5}$, (c) PVA/Chi/$Mel^{1.0}$, (d) PVA/Chi/$Mel^{2.0}$. Higher melanin content progressively darkens the films and slightly reduces transparency, consistent with melanin's intense pigmentation

with the amino groups in chitosan, indicate interactions between the polysaccharide backbone and melanin. Such interactions could impact the antimicrobial properties and biodegradability of the composite films, as chitosan's antimicrobial properties are influenced by the presence of these functional groups [61].

The bands at 1147 (C–O–C ether linkage) and 1067 cm^{-1} (C–OH stretching in the polysaccharide ring) are also significant [57,60]. The shift in these regions suggests that the melanin incorporation may alter the chemical stability and water absorption properties of the composite films, as polysaccharide structures influence film hydrophilicity and resistance to degradation [62]. In summary, the FTIR spectral shifts provide insight into how melanin incorporation affects the physical, mechanical, and functional properties of the films, including strength, flexibility, biodegradability, and antimicrobial activity, all of which are crucial for the films' applications in food packaging or biomedical fields.

Thickness and TS of The Composite Films

The thickness and TS of the PVA/Chi and PVA/Chi/Mel composite films are presented in Table 1. The film without melanin (PVA/Chi) exhibited a thickness of 0.177 ± 0.01 mm, which progressively increased with the addition of melanin. This increase in film thickness depended on the concentration of MNPs and is likely attributed to the additional solid content introduced by melanin. A higher melanin content resulted in correspondingly thicker films. Moreover, melanin incorporation also influenced the tensile strength of the films. The TS of the composite films increased significantly ($p < 0.05$) at melanin concentrations exceeding 0.5 wt.%, reflecting an enhancement in film strength. The increased TS of the PVA/Chi/Mel composite films with increasing melanin content is likely attributed to enhanced molecular interactions between the PVA/Chi matrix and the incorporated melanin. In general, both the thickness and TS of composite films are strongly influenced by the dispersion of nanofillers, as well as the intermolecular and intramolecular interactions among polymer chains within the film matrix [27].

WS and SR of Composite Films

The WS and SR of the PVA/Chi/Mel composite films are presented in Table 2. The incorporation of melanin notably influenced both WS and SR. A significant reduction in WS was observed with increasing melanin concentration, particularly at concentrations above 0.5%, where the differences were statistically significant ($p < 0.05$). This decline in solubility is likely attributed to the hydrophobic nature of melanin, which limits water interaction with the polymer matrix. Similarly, the SR of the films decreased as melanin concentration increased. The highest swelling was observed in the PVA/Chi film (145.52%), followed by PVA/Chi/$Mel^{0.5}$ (134.68%), PVA/Chi/$Mel^{1.0}$ (107.33%), and PVA/Chi/$Mel^{2.0}$ (105.12%). The reduction in SR was also statistically significant ($p < 0.05$) at melanin concentrations exceeding 0.5%, indicating the potential of melanin to enhance water resistance in the composite films [27]. The reduction in SR of the PVA/Chi/Mel composite films was likely attributed to incorporating melanin, which possessed greater hydrophobicity than the PVA/Chi matrix. A similar trend has been observed

Table 1. Thickness and TS of PVA/Chi/Mel composite films containing 0.0–2.0 wt.% melanin

Films	Thickness (mm)	TS (MPa)
PVA/Chi	0.177 ± 0.01^{a}	16.16 ± 2.51^{a}
PVA/Chi/$Mel^{0.5}$	$0.197 \pm 0.01^{a,b}$	$19.73 \pm 2.49^{a,b}$
PVA/Chi/$Mel^{1.0}$	$0.210 \pm 0.01^{b,c}$	$24.18 \pm 4.64^{b,c}$
PVA/Chi/$Mel^{2.0}$	0.230 ± 0.01^{c}	28.81 ± 1.87^{c}

Values are expressed as mean ± standard deviation. Mean values within the same column that share the same letter are not significantly different ($p > 0.05$), as determined by Tukey's test

Table 2. WS and SR of PVA/Chi/Mel composite films containing 0.0–2.0 wt.% melanin

Films	WS (%)	SR (%)
PVA/Chi	31.53 ± 1.69^{a}	145.52 ± 4.76^{a}
PVA/Chi/$Mel^{0.5}$	$29.02 \pm 1.37^{a,b}$	134.68 ± 5.97^{a}
PVA/Chi/$Mel^{1.0}$	25.75 ± 2.04^{b}	107.33 ± 7.82^{b}
PVA/Chi/$Mel^{2.0}$	24.85 ± 2.39^{b}	105.12 ± 7.29^{b}

Values are expressed as mean ± standard deviation. Means within the same column that share the same letter are not significantly different ($p > 0.05$), as determined by Tukey's test

in previous studies, where the inclusion of hydrophobic nanoparticles led to a decreased SR in agar-based films [47].

Degradability

The degradation behavior of PVA/Chi and PVA/Chi/Mel composite films over 7, 14, 21, 28, and 35 d is shown in Fig. 4. Incorporating melanin into the PVA/chitosan matrix consistently reduced mass loss compared to the neat PVA/chitosan film, with the effect becoming more pronounced at higher melanin concentrations. This reduction is attributable to several chemical and structural properties of melanin. Melanin is a heterogeneous biopolymer composed of indole and phenolic subunits rich in π-conjugated systems, which confer high radical-scavenging activity and stability against oxidative degradation [26,63]. Its ability to neutralize reactive oxygen species (ROS) and chelate transition metals can suppress oxidative and enzymatic reactions that typically accelerate polymer breakdown [64].

In the early degradation phase (day 7), microbial and enzymatic activity, along with hydrolytic and photolytic effects, drive faster mass loss [65]. The PVA/Chi film degraded by 31.43 ± 0.17%, while PVA/Chi/Mel$^{0.5}$, PVA/Chi/Mel$^{1.0}$, and PVA/Chi/Mel$^{2.0}$ showed lower values of 30.18 ± 0.67, 28.66 ± 1.59, and 27.67 ± 0.12%, respectively. Over time, the degradation rate slowed, likely due to depletion of labile components and morphological changes such as partial cross-linking or increased crystallinity in amorphous regions adjacent to crystalline domains [66], which hinders further enzymatic or hydrolytic attack [65].

By day 35, differences between films became significant: PVA/Chi degraded by 47.09 ± 1.74%, while PVA/Chi/Mel$^{0.5}$, PVA/Chi/Mel$^{1.0}$, and PVA/Chi/Mel$^{2.0}$ degraded by 46.61 ± 4.29, 46.72 ± 4.21, and 44.68 ± 1.32%, respectively. The greater stability at higher melanin loading can also be explained by its hydrophobic character, which reduces water uptake and limits hydrolytic chain scission [67-68]. Furthermore, the aromatic and crosslinked nature of melanin's macromolecular structure contributes to thermal and photostability, creating a physical barrier within the polymer matrix that impedes microbial penetration and enzymatic cleavage [20]. Overall, the chemical composition of melanin—aromatic backbones, phenolic groups, and stable crosslinked networks—along with its antioxidant and hydrophobic properties, synergistically enhances the durability of PVA/chitosan films by mitigating oxidative, hydrolytic, and enzymatic degradation pathways.

Antibacterial Activity

The growth of *E. coli* and *S. aureus* was assessed by measuring turbidity at 600 nm, and the I_f was calculated from the turbidity data across different melanin

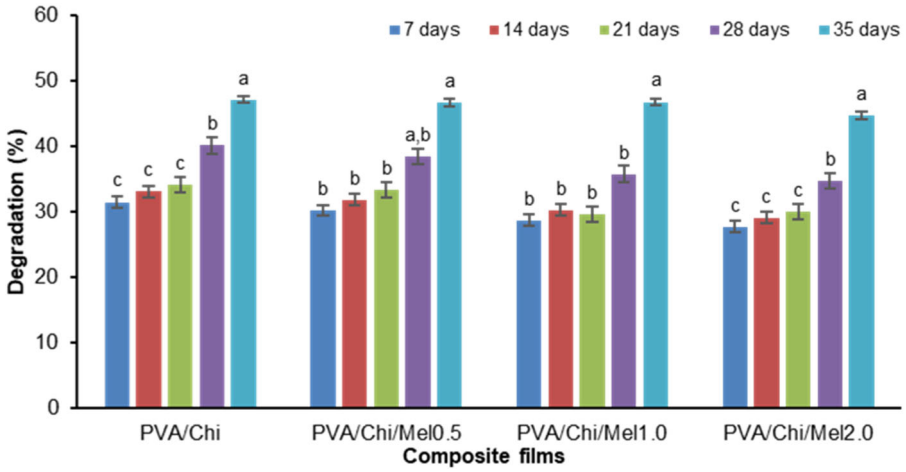

Fig 4. Degradation behavior of PVA/Chi/Mel composite films (0.0–2.0 wt.% melanin) over 7–35 d, showing reduced mass loss with higher melanin content. Values are expressed as mean ± standard deviation. Means within the same composite film that share the same letter are not significantly different ($p > 0.05$), as determined by Tukey's test

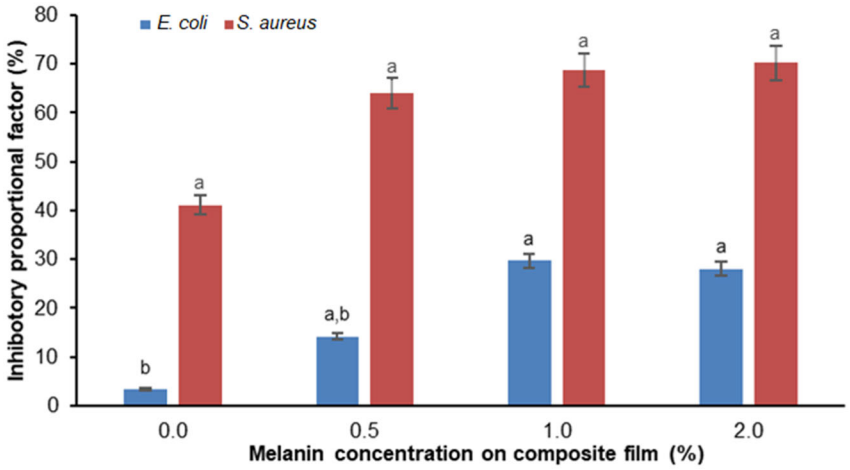

Fig 5. Inhibitory Proportional Factor (If) of PVA/Chi/Mel composite films against *E. coli* and *S. aureus* at different melanin loadings, showing higher inhibition for *S. aureus*. Values are expressed as mean ± standard deviation. Means within the same composite film that share the same letter are not significantly different ($p > 0.05$), as determined by Tukey's test

concentrations in PVA/chitosan composite films, as illustrated in Fig. 5. While both bacterial strains displayed comparable overall growth trends, *S. aureus* exhibited inhibition values about 50% higher than *E. coli* at equivalent melanin concentrations, indicating greater susceptibility of the Gram-positive strain. For both species, antibacterial activity increased in clear proportion to the melanin content in the films.

The enhanced antibacterial performance is attributed to the synergistic effects of chitosan and melanin. Chitosan's cationic amino groups interact electrostatically with negatively charged bacterial cell wall components, causing membrane disruption and leakage of intracellular contents [69-70]. Melanin, a naturally occurring pigment with antioxidant properties, enhances this effect via multiple pathways. Structurally, melanin can establish hydrophobic interactions with bacterial membranes, which are more effective against *S. aureus* due to its thick, exposed peptidoglycan layer and the absence of an outer membrane [71-72]. Functionally, melanin can generate ROS, particularly hydrogen peroxide (H_2O_2), either under physiological conditions or upon light exposure [73-74]. ROS cause oxidative damage to lipids, proteins, and nucleic acids, leading to cell death [73,75-76].

Comparative studies show that Gram-positive bacteria are generally more vulnerable to ROS-mediated damage because their peptidoglycan layer is directly exposed, whereas Gram-negative bacteria possess an additional outer membrane that limits ROS penetration [77-78]. In *S. aureus*, ROS such as H_2O_2 can cause extensive damage, including DNA degradation and broader impairment of vital cellular functions [77]. Furthermore, melanin's photothermal properties—its ability to absorb light and convert it into localized heat—can intensify oxidative stress, further amplifying antibacterial efficacy [79].

Although this study demonstrates the integration of melanin and chitosan derived from BSF into PVA-based films, it did not conduct antibacterial testing of PVA/chitosan and PVA/melanin films. Future research will focus on evaluating the antibacterial activities of these composite films to investigate further the synergistic effects of melanin and chitosan in enhancing antimicrobial properties.

■ CONCLUSION

This study fabricated PVA and chitosan-based composite films reinforced with MNPs using a straightforward solution casting method. Incorporating melanin enhanced the structural integrity, morphological characteristics, and antibacterial efficacy of the films against *E. coli* and *S. aureus*. The mechanical strength of the films showed moderate improvement with increasing melanin content, which also correlated with enhanced

antimicrobial performance. These findings demonstrate the potential of PVA–chitosan–melanin composite films as sustainable materials for antimicrobial food packaging and biomedical applications. However, this study is limited by the lack of long-term degradation analysis under real environmental conditions, which is essential for understanding the films' stability over time. Additionally, while the films exhibit good antimicrobial properties, further studies on cytocompatibility and biofunctionality are necessary to ensure their applicability in biomedical fields. Future research should evaluate the films' thermal behavior, barrier properties, and performance under actual storage conditions to support their practical implementation. Furthermore, optimizing film formulation and processing parameters will be crucial to balance mechanical strength, antimicrobial activity, and environmental degradability. This will help pave the way for scalable production and commercial viability in various applications.

■ ACKNOWLEDGMENTS

This work was supported by the Ministry of Education, Culture, Research, and Technology of the Republic of Indonesia (Grant No. 013/E5PG.02.00/PL. BATCH.2/2024; 3770/UN1/DITLIT/PT.01.03/2024) and by the Gadjah Mada University Final Project Recognition Program 2024 (Grant No. 5286/UN1.P1/PT.01.03/2024).

■ CONFLICT OF INTEREST

The authors declare no known competing financial interests or personal ties that could have influenced this paper's work.

■ AUTHOR CONTRIBUTIONS

Agus Prasetya, Joko Wintoko, Zahrul Mufrodi, Pandji Prawisudha, Kun Sri Budiasih, Abdul Rahman Siregar, and Chandra Wahyu Purnomo conceived the idea. Zainal Mustakim, Fanny Sakinah, and Chandra Wahyu Purnomo wrote and revised the manuscript. All authors agreed to the final version of this manuscript.

■ REFERENCES

[1] Moshood, T.D., Nawanir, G., Mahmud, F., Mohamad, F., Ahmad, M.H., and AbdulGhani, A., 2022, Biodegradable plastic applications towards sustainability: A recent innovations in the green product, *Cleaner Eng. Technol.*, 6, 100404.

[2] Santini, G., Zizolfi, M., Santorufo, L., Memoli, V., D'Ascoli, R., and Maisto, G., 2024, Soil microbial biomass and microarthropod community responses to conventional and biodegradable plastics, *Soil Syst.*, 8 (3), 92.

[3] Karnwal, A., Kumar, G., Singh, R., Selvaraj, M., Malik, T., and Al Tawaha, A.R.M., 2025, Natural biopolymers in edible coatings: Applications in food preservation, *Food Chem.: X*, 25, 102171.

[4] Matar, G.H., and Andac, M., 2025, Recent advances in sustainable biopolymer films incorporating vanillin for enhanced food preservation and packaging, *Polym. Bull.*, 82 (8), 2751–2777.

[5] Galstyan, A., and Strokov, K., 2022, Influence of photosensitizer concentration and polymer composition on photoinduced antimicrobial activity of PVA- and PVA-chitosan-based electrospun nanomaterials cross-linked with tailor-made silicon(IV) phthalocyanine, *Photochem. Photobiol. Sci.*, 21 (8), 1387–1398.

[6] Choo, K.W., Dhital, R., Mao, L., Lin, M., and Mustapha, A., 2021, Development of polyvinyl alcohol/chitosan/modified bacterial nanocellulose films incorporated with 4-hexylresorcinol for food packaging applications, *Food Packag. Shelf Life*, 30, 100769.

[7] Yan, J., Li, M., Wang, H., Lian, X., Fan, Y., Xie, Z., Niu, B., and Li, W., 2021, Preparation and property studies of chitosan-PVA biodegradable antibacterial multilayer films doped with Cu_2O and nano-chitosan composites, *Food Control*, 126, 108049.

[8] Alvarado, M.C., 2024, Recent progress in polyvinyl alcohol (PVA)/nanocellulose composite films for packaging applications: A comprehensive review of the impact on physico-mechanical properties, *Food Bioeng.*, 3 (2), 189–209.

[9] Hong, F., Qiu, P., Wang, Y., Ren, P., Liu, J., Zhao, J., and Gou, D., 2024, Chitosan-based hydrogels: From preparation to applications, a review, *Food Chem.: X*, 21, 101095.

[10] Assauqi, N.F., Lusiana, R.A., and Masruchin, N., 2025, Optimization of chitosan-PEG/ZnO hydrogel formulation with pomegranate peel extract as an alternative for wound healing, *Indones. J. Chem.*, 25 (3), 905–918.

[11] He, H., Wu, Z., Xiao, S., and Yin, P., 2024, Characterization of corn starch/chitosan composite films incorporated with amino-, carboxyl-, and hydroxyl-terminated hyperbranched dendrimers: A comparative study, *Int. J. Biol. Macromol.*, 283 (Pt. 1), 137573.

[12] Bernal, R.A.O., Olekhnovich, R.O., and Uspenskaya, M.V., 2023, Influence of thermal treatment and acetic acid concentration on the electroactive properties of chitosan/PVA-based micro- and nanofibers, *Polymers*, 15 (18), 3719.

[13] Liu, Y., Wang, S., Lan, W., and Qin, W., 2017, Fabrication and testing of PVA/chitosan bilayer films for strawberry packaging, *Coatings*, 7 (8), 109.

[14] He, Y., Zhang, X., Zhang, Z., Lin, B., and Yu, H., 2025, Preparation and improved properties of vanillin-crosslinked polyvinyl alcohol/chitosan active packaging films, *Molecules*, 30 (6), 1334.

[15] Sun, R., Li, L., Zhou, J., Zhang, Y., Sun, H., Zhang, D., and Wu, Q., 2025, Development of zein–PEG400/PVA–chitosan bilayer films for intelligent packaging, *Polymers*, 17 (3), 387.

[16] de Morais Mirres, A.C., Vieira, I.R., Tessaro, L., da Silva, B.D., de Andrade, J.C., da Silva, A.A., Carvalho, N.M.F., de Sousa, A.M., and Conte-Junior, C.A., 2024, Nanocomposite films of babassu coconut mesocarp and green ZnO nanoparticles for application in antimicrobial food packaging, *Foods*, 13 (12), 1895.

[17] Jafarzadeh, S., Oladzadabbasabadi, N., Dheyab, M.A., Lalabadi, M.A., Sheibani, S., Ghasemlou, M., Esmaeili, Y., Barrow, C.J., Naebe, M., and Timms, W., 2025, Emerging trends in smart and sustainable nano-biosensing: The role of green nanomaterials, *Ind. Crops Prod.*, 223, 120108.

[18] Escobar Rodríguez, C., Zaremska, V., Klammsteiner, T., Kampatsikas, I., Münstermann, N., Weichold, O., and Gruber, S., 2025, Chitosan obtained from black soldier fly larval cuticles expands the value chain and is effective as a biocontrol agent to combat plant pathogens, *Carbohydr. Polym.*, 349 (Pt. B), 123023.

[19] Chen, Y., Guo, Y., He, X., Tan, B., Liao, Z., Chen, A., Gu, X., Li, X., Chen, X., Chen, B., Lin, S., Li, W., Hu, P., Zhu, X., Zhao, W., and Niu, J., 2025, Comprehensive utilization of black soldier fly (*Hermetia illucens*) larvae: Extraction, recovery and characterization of peptide, chitin and melanin and scaling-up trial, *Sep. Purif. Technol.*, 361, 131262.

[20] Liang, Y., Zhao, Y., Sun, H., Dan, J., Kang, Y., Zhang, Q., Su, Z., Ni, Y., Shi, S., Wang, J., and Zhang, W., 2023, Natural melanin nanoparticle-based photothermal film for edible antibacterial food packaging, *Food Chem.*, 401, 134117.

[21] Sunil Kumar, B.T., Sathyendra Rao, B.V., Swathi, S., Vanajakshi, V., Hebbar, H.U., and Singh, S.A., 2024, Characterization, antioxidant, and antimicrobial activity of melanin extracted from nigerseed hulls, *Food Biosci.*, 61, 104929.

[22] Mustakim, Z., Prasetya, A., Wintoko, J., Kayati, F.N., and Purnomo, C.W., 2024, Review on melanin application as an antibacterial and antioxidant agent in food packaging, *Indones. J. Chem.*, 24 (6), 1906–1920.

[23] Liu, C., Zou, Q., Tang, H., Liu, J., Zhang, S., Fan, C., Zhang, J., Liu, R., Liu, Y., Liu, R., Zhao, Y., Wu, Q., Qi, Z., and Shen, Y., 2023, Melanin nanoparticles alleviate sepsis-induced myocardial injury by suppressing ferroptosis and inflammation, *Bioact. Mater.*, 24, 313–321.

[24] Le, T.K., Lai, S.Y., Huang, Y.W., Chen, Y.T., Hou, C.Y., and Hsieh, S.L., 2024, Antioxidant activity and mechanism of melanin from cuttlefish (*Sepia pharaonis*) ink on Clone-9 cells, *Food Biosci.*, 60, 104444.

[25] Qin, Y., and Xia, Y., 2024, Melanin in fungi: Advances in structure, biosynthesis, regulation, and metabolic engineering, *Microb. Cell Fact.*, 23 (1), 334.

[26] Guo, L., Li, W., Gu, Z., Wang, L., Guo, L., Ma, S., Li, C., Sun, J., Han, B., and Chang, J., 2023, Recent

advances and progress on melanin: From source to application, *Int. J. Mol. Sci.*, 24 (5), 4360.

[27] Roy, S., and Rhim, J.W., 2019, Agar-based antioxidant composite films incorporated with melanin nanoparticles, *Food Hydrocolloids*, 94, 391–398.

[28] Bruno, D., Orlando, M., Testa, E., Carnevale Miino, M., Pesaro, G., Miceli, M., Pollegioni, L., Barbera, V., Fasoli, E., Draghi, L., Baltrocchi, A.P.D., Ferronato, N., Seri, R., Maggi, E., Caccia, S., Casartelli, M., Molla, G., Galimberti, M.S., Torretta, V., Vezzulli, A., and Tettamanti, G., 2025, Valorization of organic waste through black soldier fly: On the way of a real circular bioeconomy process, *Waste Manage.*, 191, 123–134.

[29] Salsabila, S., Kerdpiboon, S., Kerr, W.L., and Puttongsiri, T., 2024, Drying effects on physicochemical and functional properties of cuttlefish (*Sepia officinalis*) ink powder, *J. Agric. Food Res.*, 17, 101250.

[30] Triunfo, M., Tafi, E., Guarnieri, A., Salvia, R., Scieuzo, C., Hahn, T., Zibek, S., Gagliardini, A., Panariello, L., Coltelli, M.B., De Bonis, A., and Falabella, P., 2022, Characterization of chitin and chitosan derived from *Hermetia illucens*, a further step in a circular economy process, *Sci. Rep.*, 12 (1), 6613.

[31] Bahndral, A., Shams, R., Dash, K.K., Chaudhary, P., Mukarram Shaikh, A., and Béla, K., 2025, Microwave assisted extraction of chitosan from *Agaricus bisporus*: Techno-functional and microstructural properties, *Carbohydr. Polym. Technol. Appl.*, 9, 100730.

[32] Ghanim, B., O'Dwyer, T.F., Leahy, J.J., Willquist, K., Courtney, R., Pembroke, J.T., and Murnane, J.G., 2020, Application of KOH modified seaweed hydrochar as a biosorbent of vanadium from aqueous solution: Characterisations, mechanisms and regeneration capacity, *J. Environ. Chem. Eng.*, 8 (5), 104176.

[33] Hahn, T., Egger, J., Krake, S., Dyballa, M., Stegbauer, L., von Seggern, N., Bruheim, I., and Zibek, S., 2024, Comprehensive characterization and evaluation of the process chain and products from *Euphausia superba* exocuticles to chitosan, *J. Appl. Polym. Sci.*, 141 (2), e-54789.

[34] Coltelli, M.B., Gigante, V., Panariello, L., Aliotta, L., Scieuzo, C., Falabella, P., and Lazzeri, A., 2025, Chitin and chitosan materials from black soldier fly (*Hermetia illucens*): An insight onto their thermal degradation and mechanical behavior linked to their copolymeric structure, *Polym. Test.*, 150, 108922.

[35] Liang, M., Wang, H., Zhou, Z., Huang, Y., and Suo, H., 2025, Antibacterial mechanism of *Lactiplantibacillus plantarum* SHY96 cell-free supernatant against *Listeria monocytogenes* revealed by metabolomics and potential application on chicken breast meat preservation, *Food Chem.: X*, 25, 102078.

[36] Das, P., Das, M., Sahoo, S.K., Dandapat, J., and Pradhan, J., 2025, Characterization of extracellular chitin deacetylase from *Aneurinibacillus aneurinilyticus* isolated from marine crustacean shell, *Curr. Res. Microb. Sci.*, 8, 100325.

[37] Koch, S.M., Freidank-Pohl, C., Siontas, O., Cortesao, M., Mota, A., Runzheimer, K., Jung, S., Rebrosova, K., Siler, M., Moeller, R., and Meyer, V., 2023, *Aspergillus niger* as a cell factory for the production of pyomelanin, a molecule with UV-C radiation shielding activity, *Front. Microbiol.*, 14, 1233740.

[38] Zhu, Y.K., Li, M.H., Yang, M., Xu, J.X., Ren, M.Y., Zhao, Z.K., Wang, L., Yang, J., Liu, J., and Zhang, M.W., 2025, Extraction of walnut protein using deep eutectic solvent aqueous two-phase system: Investigation of structural and functional properties, *Food Chem.: X*, 28, 102546.

[39] Wibowo, J.T., Kellermann, M.Y., Petersen, L.E., Alfiansah, Y.R., Lattyak, C., and Schupp, P.J., 2022, Characterization of an insoluble and soluble form of melanin produced by *Streptomyces cavourensis* SV 21, a sea cucumber associated bacterium, *Mar. Drugs*, 20 (1), 54.

[40] Abd El-Aziz, S.M., Faraag, A.H.I., Ibrahim, A.M., Albrakati, A., and Bakkar, M.R., 2024, Tyrosinase

enzyme purification and immobilization from *Pseudomonas* sp. EG22 using cellulose coated magnetic nanoparticles: Characterization and application in melanin production, *World J. Microbiol. Biotechnol.*, 40 (1), 10.

[41] Garavand, Y., Taheri-Garavand, A., Garavand, F., Shahbazi, F., Khodaei, D., and Cacciotti, I., 2022, Starch-polyvinyl alcohol-based films reinforced with chitosan nanoparticles: Physical, mechanical, structural, thermal and antimicrobial properties, *Appl. Sci.*, 12 (3), 1111.

[42] Momtaz, F., Momtaz, E., Mehrgardi, M.A., Momtaz, M., Narimani, T., and Poursina, F., 2024, Enhanced antibacterial properties of polyvinyl alcohol/starch/chitosan films with NiO–CuO nanoparticles for food packaging, *Sci. Rep.*, 14 (1), 7356.

[43] Rajasekaran, B., Singh, A., Ponnusamy, A., Patil, U., Zhang, B., Hong, H., and Benjakul, S., 2023, Ultrasound treated fish myofibrillar protein: Physicochemical properties and its stabilizing effect on shrimp oil-in-water emulsion, *Ultrason. Sonochem.*, 98, 106513.

[44] Yuan, J., Ran, M., Zhou, X., Zhu, P., Liu, L., Jiang, R., and Zhou, X., 2024, The impact of heterogeneity of aggregates coated with asphalt mortar on their FTIR spectra and spectral reproducibility, *Appl. Sci.*, 14 (13), 5857.

[45] Grasso, M., Petrov, V., and Manera, A., 2024, Accuracy and error analysis of optical liquid film thickness measurement with total internal reflection method (TIRM), *Exp. Fluids*, 65 (6), 83.

[46] Roy, S., and Rhim, J.W., 2020, Preparation of carbohydrate-based functional composite films incorporated with curcumin, *Food Hydrocolloids*, 98, 105302.

[47] Shankar, S., and Rhim, J.W., 2017, Preparation and characterization of agar/lignin/silver nanoparticles composite films with ultraviolet light barrier and antibacterial properties, *Food Hydrocolloids*, 71, 76–84.

[48] Eskandari, Z., Osanloo, M., Mazloomi, S.M., Zarenezhad, E., Mollakhalili-Meybodi, N., and Nematollahi, A., 2025, Bioactive edible films for chicken breast packaging: Integration of chia seed mucilage with nanoemulsions of *Cinnamomum zeylanicum* and *Satureja khuzestanica*, *Appl. Food Res.*, 5 (1), 100959.

[49] Alshabanat, M., 2019, Morphological, thermal, and biodegradation properties of LLDPE/treated date palm waste composite buried in a soil environment, *J. Saudi Chem. Soc.*, 23 (3), 355–364.

[50] Sultan, A., Sultan, H., Shahzad, W., Kareem, A., Liaqat, A., Ashraf, Z., Shahid, A., Rauf, A., Saeed, S., Mehmood, T., Zahra, M., Soto-Bubert, A., and Acevedo, R., 2024, Comparative analysis of physical and mechanical properties of starch based bioplastic derived from the pulp and peel of potatoes, *J. Indian Chem. Soc.*, 101 (10), 101301.

[51] Goy, R.C., Morais, S.T.B., and Assis, O.B.G., 2016, Evaluation of the antimicrobial activity of chitosan and its quaternized derivative on *E. coli* and *S. aureus* growth, *Rev. Bras. Farmacogn.*, 26 (1), 122–127.

[52] Afrin, S., Tamanna, T., Shahajadi, U.F., Bhowmik, B., Jui, A.H., Miah, M.A.S., and Bhuiyan, M.N.I., 2024, Characterization of protease-producing bacteria from garden soil and antagonistic activity against pathogenic bacteria, *Microbe*, 4, 100123.

[53] Wacogne, B., Belinger Podevin, M., Vaccari, N., Koubevi, C., Codjiová, C., Gutierrez, E., Davoine, L., Robert-Nicoud, M., Rouleau, A., and Frelet-Barrand, A., 2024, Concentration vs. optical density of ESKAPEE bacteria: A method to determine the optimum measurement wavelength, *Sensors*, 24 (24), 8160.

[54] Poulose, N., Sajayan, A., Ravindran, A., Sreechithra, T.V., Vardhan, V., Selvin, J., and Kiran, G.S., 2020, Photoprotective effect of nanomelanin-seaweed concentrate in formulated cosmetic cream: With improved antioxidant and wound healing properties, *J. Photochem. Photobiol., B*, 205, 111816.

[55] Tan, Y., Liu, X., Cheng, Z., Zhan, Q., and Zhao, L., 2024, Preparation and characterization of bio-based freshness indicator labels loaded with natural pigments with high stability and sensitivity, *Foods*, 13 (24), 4049.

[56] Yang, Y., Fu, J., Duan, Q., Xie, H., Dong, X., and Yu, L., 2024, Strategies and methodologies for improving toughness of starch films, *Foods*, 13 (24), 4036.

[57] Ruiz Matute, A.I., Cardelle-Cobas, A., García-Bermejo, A.B., Montilla, A., Olano, A., and Corzo, N., 2013, Synthesis, characterization and functional properties of galactosylated derivatives of chitosan through amide formation, *Food Hydrocolloids*, 33 (2), 245–255.

[58] Wu, J., Wang, M.J., and Stark, J.P.W., 2006, Evaluation of band structure and concentration of ionic liquid $BMImBF_4$ in molecular mixtures by using second derivatives of FTIR spectra, *J. Quant. Spectrosc. Radiat. Transfer*, 102 (2), 228–235.

[59] Kivilcim, F.N., 2025, Heat treatment impacts on film morphology in biaxially oriented polypropylene films, *Food Sci. Nutr.*, 13 (6), e70458.

[60] Kumar, S., Ye, F., Mazinani, B., Dobretsov, S., and Dutta, J., 2021, Chitosan nanocomposite coatings containing chemically resistant ZnO–SnO_x core–shell nanoparticles for photocatalytic antifouling, *Int. J. Mol. Sci.*, 22 (9), 4513.

[61] Ferreira, P.G., Ferreira, V.F., da Silva, F.C., Freitas, C.S., Pereira, P.R., and Paschoalin, V.M.F., 2022, Chitosans and nanochitosans: Recent advances in skin protection, regeneration, and repair, *Pharmaceutics*, 14 (6), 1307.

[62] Marasinghe, W.N., Jayathunge, K.G.L.R., Dassanayake, R.S., Liyanage, R., Bandara, P.C., Rajapaksha, S.M., and Gunathilake, C., 2024, Structure, properties, and recent developments in polysaccharide- and aliphatic polyester-based packaging—A review, *J. Compos. Sci.*, 8 (3), 114.

[63] Mavridi-Printezi, A., Menichetti, A., Mordini, D., and Montalti, M., 2023, Functionalization of and through melanin: Strategies and bio-applications, *Int. J. Mol. Sci.*, 24 (11), 9689.

[64] Tumilaar, S.G., Hardianto, A., Dohi, H., and Kurnia, D., 2023, A comprehensive review of free radicals, oxidative stress, and antioxidants: Overview, clinical applications, global perspectives, future directions, and mechanisms of antioxidant activity of flavonoid compounds, *J. Chem.*, 2024 (1), 5594386.

[65] Sutkar, P.R., Gadewar, R.D., and Dhulap, V.P., 2023, Recent trends in degradation of microplastics in the environment: A state-of-the-art review, *J. Hazard. Mater. Adv.*, 11, 100343.

[66] Chamas, A., Moon, H., Zheng, J., Qiu, Y., Tabassum, T., Jang, J.H., Abu-Omar, M., Scott, S.L., and Suh, S., 2020, Degradation rates of plastics in the environment, *ACS Sustainable Chem. Eng.*, 8 (9), 3494–3511.

[67] García-García, M., Jaime-Ferrer, J.S., Medrano-Lango, F.N., Quintana-Rodríguez, E., Campos-García, T., Rodríguez-Sevilla, E., and Orona-Tamayo, D., 2025, Electrospun membranes loaded with melanin derived from pecan nutshell (*Carya illinoinensis*) residues for skin-care applications, *Membranes*, 15 (2), 44.

[68] Li, B., Mei, H., Zhou, Z., Yang, J., Zhang, Y., and Qi, F., 2024, The main causes and corresponding solutions of skin pigmentation in the body, *J. Dermatol. Sci. Cosmet. Technol.*, 1 (2), 100020.

[69] Yadav, H., Malviya, R., and Kaushik, N., 2024, Chitosan in biomedicine: A comprehensive review of recent developments, *Carbohydr. Polym. Technol. Appl.*, 8, 100551.

[70] Tan, R., Li, F., Zhang, Y., Yuan, Z., Feng, X., Zhang, W., Liang, T., Cao, J., De Hoop, C.F., Peng, X., and Huang, X., 2021, High-performance biocomposite polyvinyl alcohol (PVA) films modified with cellulose nanocrystals (CNCs), tannic acid (TA), and chitosan (CS) for food packaging, *J. Nanomater.*, 2021 (1), 4821717.

[71] Łopusiewicz, Ł., Jedra, F., and Mizieińska, M., 2018, New poly(lactic acid) active packaging composite films incorporated with fungal melanin, *Polymers*, 10 (4), 386.

[72] Xu, C., Li, J., Yang, L., Shi, F., Yang, L., and Ye, M., 2017, Antibacterial activity and a membrane damage mechanism of *Lachnum* YM30 melanin against *Vibrio parahaemolyticus* and *Staphylococcus aureus*, *Food Control*, 73, 1445–1451.

[73] Aqlinia, M., Astuti, R.I., Prastya, M.E., and Wahyudi, A.T., 2025, Antioxidant potential of melanin pigment from marine sponge-associated

actinomycete *Micromonospora* sp., *J. Appl. Pharm. Sci.*, 15 (4), 212–224.

[74] Zhong, Y., Ma, T., Fu, Z., Chen, A., Yu, J., Huang, Y., and Fu, J., 2023, Effects of hydrogen peroxide-induced oxidative stress on intestinal morphology, redox status, and related molecules in squabs, *Animals*, 13 (4), 749.

[75] Liu, L., Li, S., Zhu, W., Bao, Q., Liang, Y., Zhao, T., Li, X., and Zhou, J., 2024, Study on the mechanism of ROS-induced oxidative stress injury and the broad-spectrum antimicrobial performance of nickel ion-doped V_6O_{13} powder, *Sci. Rep.*, 14 (1), 22374.

[76] Jena, A.B., Samal, R.R., Bhol, N.K., and Duttaroy, A.K., 2023, Cellular Red-Ox system in health and disease: The latest update, *Biomed. Pharmacother.*, 162, 114606.

[77] Rahmani Eliato, T., Smith, J.T., Tian, Z., Kim, E.S., Hwang, W., Andam, C.P., and Kim, Y.J., 2021, Melanin pigments extracted from horsehair as antibacterial agents, *J. Mater. Chem. B*, 9 (6), 1536–1545.

[78] Breijyeh, Z., Jubeh, B., and Karaman, R., 2020, Resistance of Gram-negative bacteria to current antibacterial agents and approaches to resolve it, *Molecules*, 25 (6), 1340.

[79] Yue, Y., and Zhao, X., 2021, Melanin-like nanomedicine in photothermal therapy applications, *Int. J. Mol. Sci.*, 22 (1), 399.